Deutsches Zentrum
für Luft- und Raumfahrt

Title:
From Scaled Experiments of Mechatronic Guidance to Multibody Simulations of DLR's Next Generation Train Set

Authors:
Andreas Heckmann, Daniel Lüdicke, Gustav Grether and Alexander Keck

Book:
Dynamics of Vehicles on Roads and Tracks: Proceedings of the 25th International Symposium on Dynamics of Vehicles on Roads and Tracks (IAVSD 2017), 14-18 August 2017, Rockhampton, Queensland, Australia

Editors:
Maksym Spiryagin, Timothy Gordon, Colin Cole, Tim McSweeney

Copyright Notice:

Citation Notice:

Andreas Heckmann, Daniel Lüdicke, Gustav Grether and Alexander Keck: From Scaled Experiments of Mechatronic Guidance to Multibody Simulations of DLR's Next Generation Train Set, In Dynamics of Vehicles on Roads and Tracks: Proceedings of the 25th International Symposium on Dynamics of Vehicles on Roads and Tracks (IAVSD 2017), CRC Press, 2017.

From Scaled Experiments of Mechatronic Guidance to Multibody Simulations of DLR's Next Generation Train Set

Andreas Heckmann, Daniel Lüdicke, Gustav Grether and Alexander Keck
Institute of System Dynamics and Control, German Aerospace Center (DLR)

ABSTRACT: The paper presents the progress of control development for mechatronic guidance within the DLR-internal project Next Generation Train. It reports on the implementation of the control on the experimental running gear hardware operated at the scale 1:5 roller rig at DLR. The state feedback control synthesis utilizes the parameter space approach in order to explicitly consider varying conicities. A feed-forward controller is introduced by model inversion. The resulting control performance is demonstrated by measurements. Then, the approach is transferred and applied to a full scale multibody model of the NGT train set. Specific measures are required to account for gyroscopic effects in transition curves, where the superelevation of the track is in- or decreasing. Simulation results document the achievements of the control design and validate the underlying considerations.

1 INTRODUCTION

The DLR-internal, long-term research project Next Generation Train (NGT) considers a very high speed train running at 400 km/h in daily operation. A double deck configuration and light-weight design have been chosen in order to reduce life-cycle-costs and energy consumption per passenger. The intermediate wagons run on two single wheel pairs, while the train heads employ two double-axle running gears as well consisting of independently rotating and driven wheels (IRW). This design offers the capability of almost perfect steering along curves and facilitates continuous floors even on the lower level of the double deck car body, which would have to be stepped for a conventional wheel set axle.

However as a result, the task of guidance along the track relies on active control of the IRW which therefore is a research focus of the NGT project. On the one hand a 1:5 scale experimental running gear has been constructed, see Figure 1, on the other hand a full scale multibody model of the NGT train set is established that both serve as an environment for control development.

While in (Heckmann et al., 2016), the model based control design concept for the experimental running gear has been introduced, this paper presents the implementation of the control on the hardware in Section 2. Section 3 adresses the control design for the multibody model and comments on multibody simulation results that document the enhancements compared to (Kurzeck et al., 2014). The final Section 4 concludes the paper and gives an outlook.

2 SCALED EXPERIMENTAL RUNNING GEAR

2.1 *Hardware*

The experimental running gear that was built in hardware, see Figure 1, runs on the 1:5 scaled roller rig of DLR. Its major components are the central frame, the two axle bridges, and the four wheels.

Each wheel is equipped with an in-wheel drive, namely a permanent magnet synchronous motor. The actuating torques τ_i, $i \in \{f, r\}$, where f denotes front and r rear, are applied to the wheels of each axle configuration in a differential manner, i.e. $\tau_{ij} = \pm\tau_i$, $j \in \{r, l\}$, where r signifies right and l left.

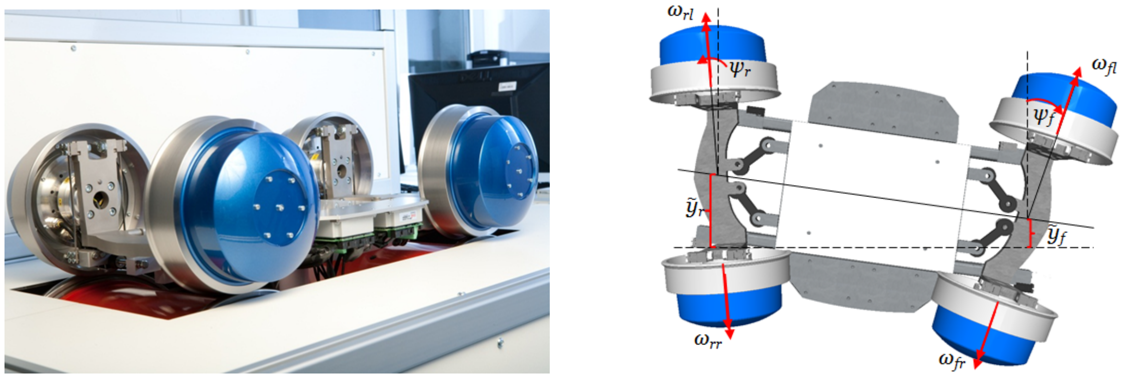

Figure 1. Experimental running gear on the 1:5 scale roller rig (left) and a schematic top view with controlled degrees of freedom with exaggerated deflections (right). see (Keck et al., 2017).

The top view to the right in Figure 1 visualizes the mechanical degrees of freedom which are relevant for mechatronic guidance. These are the lateral displacements y_f and y_r of the center points of the front and rear axle bridge with respect to the railroad centerline, the yaw angle of each axle bridge ψ_f and ψ_r and the four angular wheel velocities ω_{fr}, ω_{fl}, ω_{rl} and ω_{rr}.

As a first step the parameters of the experimental running gear were identified. In particular the stiffness associated to the rotation of each axle bridge, the actual transmission behavior of the wheel drives and the parameters of the *Polach* wheel-rail contact model (Polach, 2005) were determined by comparison of the frequency response functions

$$H(j\omega) = \frac{\mathcal{F}\{y_i(t)\}}{\mathcal{F}\{\tau_i(t)\}} \,, \qquad \mathcal{F}\{f(t)\} := \int_{-\infty}^{\infty} f(t) e^{j\omega t} \mathrm{d}t \,, \tag{1}$$

of the experimental running gear and of the simulation model on which the control design is based. Since the open-loop plant is an unstable system, already the parameter identification task required an operational initial control. Figure 2 presents the final result of the optimization process, see (Keck et al., 2017).

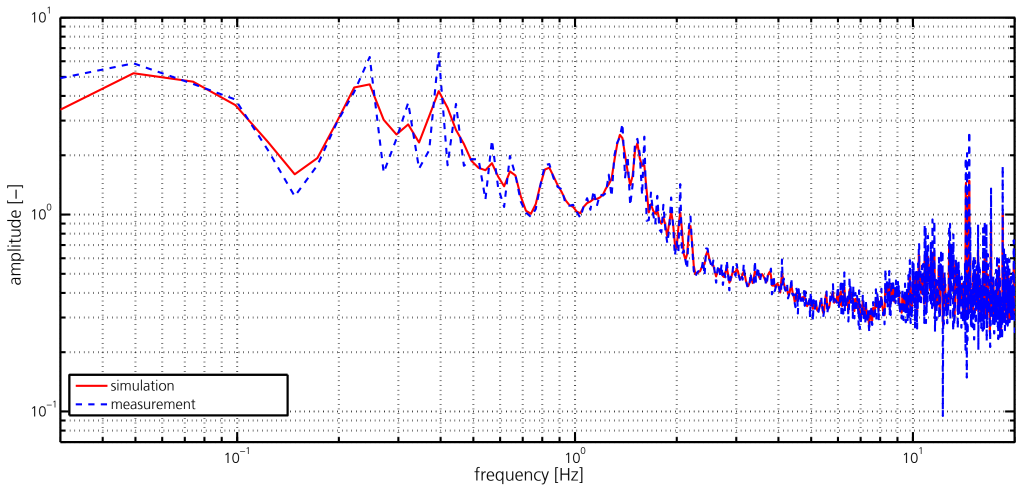

Figure 2. Comparison of the amplitude of $H(j\omega)$, see (1), as a result of the closed loop parameter identification of the experimental running gear in the frequency domain, see (Keck et al., 2017)

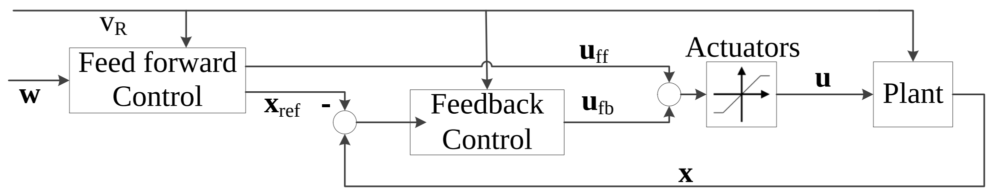

Figure 3. Structure of the experimental running gear control.

2.2 *Control Synthesis*

The control structure to implement is a result of previous work in (Heckmann et al., 2016) and shown in Figure 3. Since the system characteristics strongly depends on the running velocity v_R, the feedback control law follows a gain scheduling approach and reads

$$\tau_i = \left[k_y(v_R), k_\psi(v_R), k_{\dot\psi}(v_R) \right] \begin{bmatrix} y_i \\ \psi_i \\ \dot\psi_i \end{bmatrix} , \tag{2}$$

where k_y, k_ψ and $k_{\dot\psi}$ introduce feedback-coefficients. The model-based control synthesis explicitly takes into account that relevant system parameters such as the equivalent conicity are uncertain and change transiently. As an example, the left hand side of Figure 4 presents the boundaries of the stable regions for the feedback gain $k_y = k_y(v_R)$ for two conicities in the parameter space (Ackermann, 2012) in the left hand side plot. As long as the feedback gain remains within the intersecting area of both stability regions as given for the chosen feedback gain drawn in solid line, the control is stable and therefore robust against parameter changes.

Since a linear analysis of the so-called *analytical model* in (Heckmann et al., 2016) revealed that the transfer functions of the outputs y_i as a function of the inputs τ_i to do not comprise invariant zeros of the running gear dynamics lying in the right complex half-plane, the model can be inverted in Modelica and used in the feed-forward path in Figure 3, cf. (Thümmel et al., 2005).

2.3 *Results*

Compared to the passive wheel-set, where the rotational speed of both wheels are coupled due to the rigid shaft connection, the open-loop IRW system does not expose self-curving and centering properties. Therefore, the control development of the IRW is targeted on two tasks, on steering which describes a low-frequency action in response to curves, and on guidance which defines the operation to directly follow the track, or more accurately the centerline of the track even

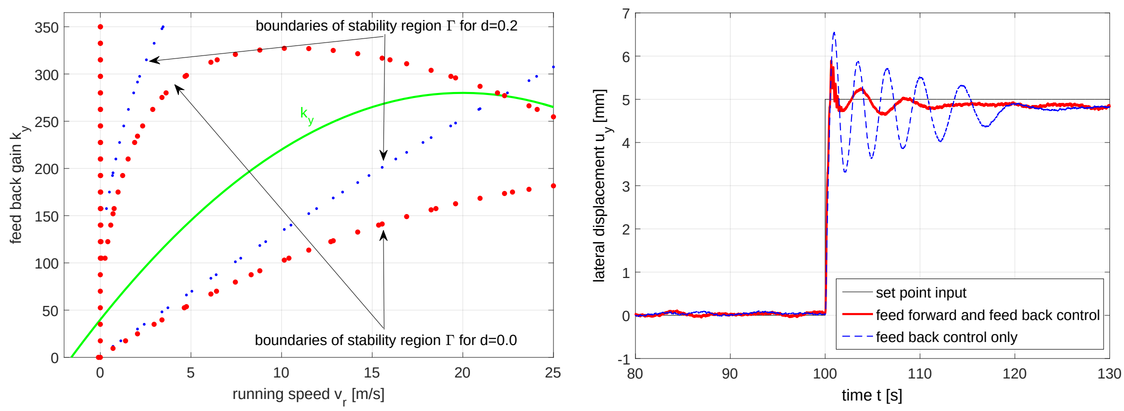

Figure 4. Parameter space synthesis of the feedback control gain $k_y(v_R)$ and step response of the experimental running gear control for $v_R = 4.7$ m/s.

in the presence of inevitable track irregularities, cf. (Goodall et al., 2006). Neither curves, nor misaligned rails are conditions that can be reproduced at the roller rig, but are to be addressed in the following section.

That is why the performance of the experimental gunning gear control on the roller rig is demonstrated using a step function from $y_i = 0\,\text{mm}$ to $y_i = 5\,\text{mm}$ as set-point input, see the right hand side plot in Figure 4. The two measured curves compare the system response for two configurations, with and without feed-forward contribution to the actuation torques τ_i. Both responses are stable, but the improvement of the dynamical set-point response due to the feed-forward contribution is obvious.

However, both results display a residual steady state error. In daily operation, running gear systems are permanently excited by track irregularities so that a stationary state is hard to achieve anyway. As long as no flange contact associated to severe wear conditions occurs it is as well not crucial to hold a precise position relative to the track centerline. Therefore, steady state accuracy is not a control design objective.

3 MULTIBODY SIMULATIONS OF THE NGT TRAIN SET

In the second branch of the development task, extensive multibody simulations as visualized in Figure 5 are used to evaluate and optimize the guidance control of the IRW as part of the NGT train set. On the one hand the transfer of the control from the scaled experimental hardware to the full scale multibody model requires to adapt geometric and mechanic parameters. On the other hand, the multibody simulation offers the capability to consider complex application scenarios with e.g. different curve radii, superelevations and rail irregularities. In this way, operational properties of the actively controlled IRW running gears such as the reduction of wear in relation to the maximum available actuator torques can be explored, cf. (Kurzeck et al., 2014).

3.1 *Robust Control Synthesis*

The control synthesis for the multibody models of the IRW corresponds to the approach introduced in (Heckmann et al., 2016) and applied in the Section 2.2, except of three items: (i) the *design model* (Heckmann et al., 2016) is extended by a passive damper with damping coefficient $k_d = 3 \cdot 10^4 \, \frac{Nms}{rad}$, which improves the control performance at high velocities; (ii) the parameters of the *design model* are adapted to scale 1:1 and (iii) the equivalent conicity as uncertain parameter is assumed to vary in the range of $d = [0.1, 0.3]$.

Stability as shown in the right hand side plot in Figure 5 and appropriate wear reduction is achieved with the following gain scheduled control parameter in the whole operating range of the longitudinal velocity v_R:

$$\tau_i = (-0.0117\, v_R^3 + 6.53\, v_R^2 - 896.3\, v_R + 5 \cdot 10^4) \cdot y_i + 3 \cdot 10^4 \cdot \psi_i + (300 + 9\, v_R) \cdot \dot{\psi}_i \,. \quad (3)$$

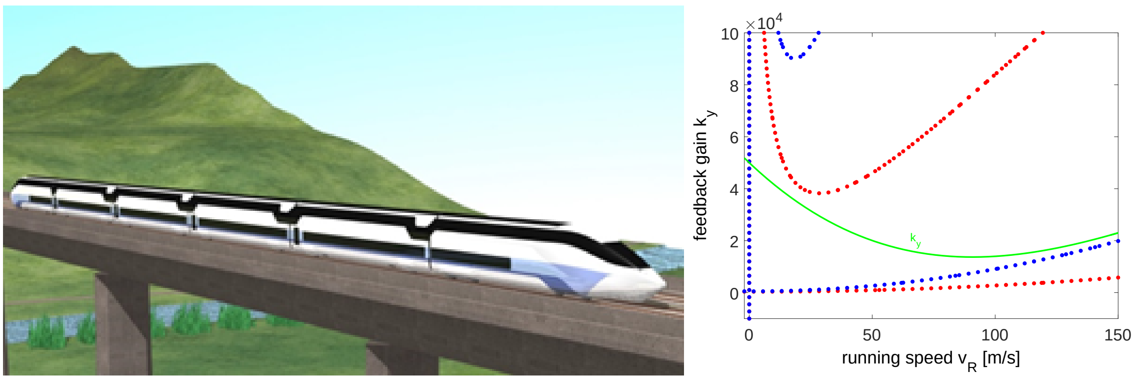

Figure 5. Animation of the NGT multibody simulation model and parameter space synthesis of the feedback control gain $k_y(v_R)$.

3.2 *Influences of Curved Tracks and Feed-forward Control*

(Kurzeck et al., 2014) includes a discussion on the impact of superelevations on the control action of IRW at very high speed that may be summarized as follows: there are relevant gyroscopic effects in transition curves, where the superelevation of the track is in- or decreasing. This effects require large values of the control action τ_i to be compensated. They scale with the moment of inertia J around the rotation axis that are affected by the large wheel diameter of 1.25 m considered in (Kurzeck et al., 2014). With this background, the wheel diameter of the current NGT IRW has been reduced to 0.98 m.

As stated above, one of the two main control objectives refers to the steering task in response to curves. It is consequently reasonable to explicitly consider curving as a part of the control design. To this aim, an analytical three mass model of an IRW is deduced, whereby a constant track radius r_T, constant longitudinal velocity v_R, a superelevation angle φ_T and its derivative $\dot{\varphi}_T$ are considered, see (Grether, 2017). Unlike to Section 2.2, this model could not be inverted with respect to the inputs v_R, r_T, φ_T and $\dot{\varphi}_T$ in order to provide a stable feed-forward control law, so far.

Hence, the further discussion is based on an analytical analysis. All time derivatives of states are set to zero and the equations are linearized in $y_i = \psi_i = \varphi_T = \dot{\varphi}_T = 0$, $\omega_{ij} = \frac{-v_R}{r_0 r_T}(r_T \mp b)$, so that the equilibrium equation for the yaw angle ψ_i yields*

$$\left(\frac{2\Lambda b^2}{r_0} y_i + \frac{b r_0}{v_R}(\omega_{il} - \omega_{ir}) + 2\frac{b^2}{r_T}\right) c_{11} + \left(\frac{2 b c_{23} d^3}{r_0} - bdgm + k_c\right)\psi_i - \frac{2 J v_R}{r_0}\dot{\varphi}_T = 0 \; , \quad (4)$$

while the equations for the wheel rotations read

$$\left(\frac{\Lambda b v_R}{r_T}(b \mp r_T) y_i + r_0^2 \omega_{ij} + (\mp b + r_T)\frac{r_0 v_R}{r_T}\right)\frac{c_{11}}{v_R} + \frac{J \dot{\varphi}_T v_R}{r_T} \mp \tau_i = 0 \, . \quad (5)$$

Solving (5) for $\omega_{ij}(y_i, \tau_i)$ and inserting the solution into (4) leads to

$$\left(-2bd^3\frac{c_{23}}{r_0} + bdgm - k_c\right)\psi_i + \frac{2 J v_R}{r_0}\dot{\varphi}_T + \frac{2b}{r_0}\tau_i = 0 \; . \quad (6)$$

Focusing on high velocities v_R, the gyroscopic moment $M_G = \frac{2 J v_R \dot{\varphi}_T}{r_0}$ in (6) associated to the change of the superelevation angle $\dot{\varphi}_T$ in transition curves becomes dominant. Furthermore, the equilibrium in ψ_i is independent of y_i, so that a specific set-point trajectory in transition curves can not be derived. An additional quantitative analysis shows that M_G cannot be compensated by yaw angles ψ_i in a valid range. This motivates a feed-forward control to compensate the gyroscopic moments with a wheel torque of $\Delta\tau_i = -\frac{J v_R \dot{\varphi}_T}{b r_0}$.

3.3 *Results*

In order to present the performance of the control including feed-forward and feedback path, a multibody simulation of the NGT train set running through the first transition to the S-curve called *Test Track 3* in (Kurzeck et al., 2014) with $r_T = 8500$ m and $v_R = 400$ km/h was performed. The left hand side plot in Figure 6 depicts the lateral position of an IRW center of an intermediate NGT car in relation to the track gauge clearance or track channel.

The transition curve starts at the longitudinal distance of $s = 260$ m. The superelevation rate is $\dot{\varphi}_T = 2.5 \cdot 10^{-2}$ rad/s and here is assumed to be known from a priori known track data or from observations of the preceding running gears.

The behavior without feed-forward contribution $\Delta\tau_i$ is characterized by almost permanent flange contact in the transition curve, cf. (Kurzeck et al., 2014, Figure 5), but occurs only incidentally if $\Delta\tau_i$ is superimposed in order to compensate the gyroscopic effects. The total control effort

*

Abbreviation	Description	Abbreviation	Description
Λ	$\frac{d}{b - r_0 d}$	b	half track gauge
r_0	nominal wheel radius	c_{ij}	extended Kalker coefficients
g	gravity	m	mass axle beam and both wheels
k_c	yaw stiffness	k_d	yaw damping

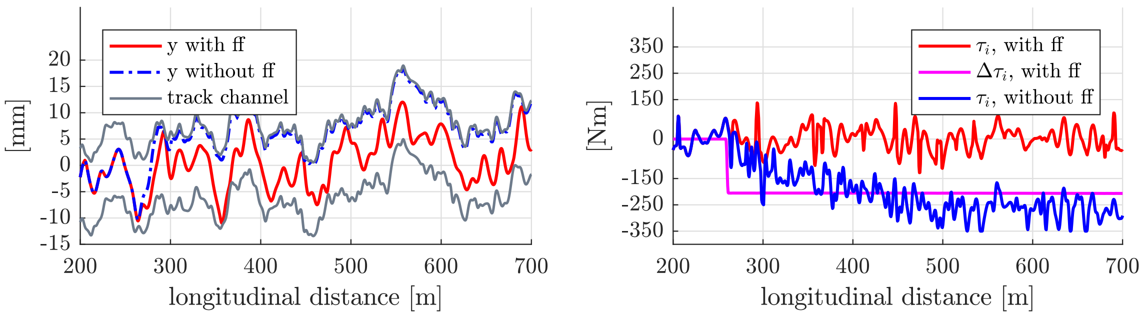

Figure 6. Guidance control with and without feed-forward contribution.

$\tau_i + \Delta\tau_i$ is limited to the $\pm 350\,$Nm, since the wheel drives additionally need capacity to provide the required traction effort.

4 CONCLUSIONS AND OUTLOOK

Two environments are employed in order to develop control for mechatronic guidance within the DLR-internal project Next Generation Train. An experimental running gear operating at a scale 1:5 roller rig including an XPCtarget rapid prototype system provides an experimental setting to design, test and validate the control. A full scale multibody simulation environment of the NGT train allows for the consideration of complex application scenarios with e.g. different curve radii, superelevations and rail irregularities. The paper presents the control synthesis approach used in both environments and demonstrates current achievements by measurements or simulation results, respectively.

Future work will address the observer design for the lateral position of the IRW with respect to the track centerline and an approach to estimate track irregularities of a preceding or leading running gear. Based on model inversion, this information will be used to generate a feed-forward control contribution for the trailing IRWs.

Besides the parameter space approach, numerical optimization will be used for control synthesis to improve robustness and to compromise actuation effort and wear reduction in the future.

REFERENCES

Ackermann, J. 2012. *Robust control: the parameter space approach*. Springer Science & Business Media.

Goodall, R. M., Bruni, S., and Mei, T. X. 2006. Concepts and prospects for actively controlled railway running gear. *Vehicle System Dynamics*, 44(sup1):60–70.

Grether, G. 2017. Dynamics of a running gear with IRWs on curved tracks for a robust control development. *PAMM*. accepted for publication.

Heckmann, A., Schwarz, C., Bünte, T., Keck, A., and Brembeck, J. 2016. Control development for the scaled experimental railway running gear of DLR. In Rosenberger, M., Plöchl, M., Six, K., and Edelmann, J., editors, *24th Symposium of the International Association for Vehicle System Dynamics (IAVSD 2015)*, volume 1 of *The Dynamics of Vehicles on Roads and Tracks*. CRC Press 2016.

Keck, A., Schwarz, C., and Heckmann, A. 2017. Parameter identication of a scaled running gear. *Mechatronics*. submitted for review.

Kurzeck, B., Heckmann, A., Wesseler, C., and Rapp, M. 2014. Mechatronic track guidance on disturbed track: the trade-off between actuator performance and wheel wear. *Vehicle System Dynamics*, 52(sup1):109–124.

Polach, O. 2005. Creep forces in simulations of traction vehicles running on adhesion limit. *Wear*, 258(7):992–1000.

Thümmel, M., Looye, G., Kurze, M., Otter, M., and Bals, J. 2005. Nonlinear inverse models for control. In *Proceedings of the 4th International Modelica Conference*, pages 267–279.